Edinburgh Research Explorer

Linking Microbial Decomposition to Dissolved Organic Matter Composition in the Revegetation of the Red Soil Erosion Area

Linking Microbial Decomposition to Dissolved Organic Matter Composition in the Revegetation of the Red Soil Erosion Area

Wenxin Chen [1,2], Huaying Hu [1], Kate Heal [3], Saran Sohi [3,4], Mulualem Tigabu [5], Weijuan Qiu [2] and Chuifan Zhou [1,2,*]

[1] College of Forestry, Fujian Agriculture and Forestry University, Fuzhou 350002, China
[2] National Positioning Observation Research Station of Red Earth Hilly Ecosystem in Changting, Longyan 366300, China
[3] School of GeoSciences, The University of Edinburgh, King's Buildings, Edinburgh EH9 3FF, UK
[4] UK Biochar Research Centre, The University of Edinburgh, Edinburgh EH9 3FF, UK
[5] Southern Swedish Forest Research Centre, Swedish University of Agricultural Sciences, P.O. Box 49, SE-230 53 Alnarp, Sweden
[*] Correspondence: zhouchuifan@163.com

Abstract: Studying the changes and linkages between dissolved organic matter (DOM) and microorganisms in soils during vegetation restoration will help to understand the role of vegetation restoration in soil carbon sequestration and thus improve the understanding of the global soil carbon cycle. Soil DOM molecules were characterized by Fourier-transform ion cyclotron resonance mass spectrometry (FT-ICR MS) and the results showed that the soil DOM consisted mainly of lignin/carboxylic rich alicyclic molecule (CRAM)-like structures, while the ratios of lipids and aliphatic/protein decreased in sequence with recovery time. Lipids and aliphatic/proteins with high H/C DOM (labile DOM) degrade preferentially, while lignin/CRAM-like structures and tannins with low H/C DOM (recalcitrant DOM) are recalcitrant during vegetation restoration. With the restoration of vegetation, DOM molecules tend to be diversified and complicated, and DOM compounds with low double bond equivalent (DBE), low aromatic, and low alkyl structures will be converted into persistent organic matter with high carbon numbers and high DBE. The diversity of soil microorganisms was determined by high-throughput sequencing. The results showed that the abundance and diversity of soil bacteria increased significantly after revegetation, while the abundance and diversity of soil fungi began to increase when the ecosystem became a more mature coniferous forest. The soil microbial community exhibited complex connectivity and strong interaction with DOM molecules during vegetation restoration. As most of the DOM molecules are recalcitrant, vegetation restoration facilitates C sequestration in the soil, thereby contributing to climate change mitigation.

Keywords: soil dissolved organic matter; bacteria; fungi; vegetation restoration

1. Introduction

Soil is vital in the carbon cycle, containing approximately three times more carbon than plants and twice as much as the atmosphere, so small changes in the soil carbon pool can cause large changes in the carbon pool [1]. However, soils may face huge carbon losses due to human activities and there is a growing interest in vegetation restoration in order to mitigate this phenomenon and promote soil carbon sequestration. This measure can increase soil carbon stocks by preventing soil erosion, increasing organic matter input, and reducing microbial decomposition [1,2].

Although dissolved organic matter (DOM) makes up only a small proportion of total soil organic matter (SOM) (<0.25%), it is extremely mobile and active in the soil and can be bioavailable [3]. DOM is ubiquitous in terrestrial ecosystems and is an important component of the global carbon cycle [4,5]. Its content and quality play an important role in regulating soil respiration, plant growth, microbial metabolism, and nutrient cycling [6].

Characterizing the composition and diversity of DOM at the molecular level, and the factors that influence DOM, and thus understanding the dynamics of soil carbon during vegetation restoration, can contribute to a better understanding of the global carbon cycle [7]. The use of ultrahigh resolution mass spectrometry (electrospray ionization Fourier-transform ion cyclotron resonance mass spectrometry, ESI-FT-ICR-MS) facilitates analysis of the detailed chemistry of DOM based on individual molecular formulae, aiding the interpretation of molecular DOM patterns across systems.

Soil microorganisms are drivers of soil carbon cycling and sequestration, and play an important role in soil development and nutrient cycling, exhibiting a high degree of structural, genetic, and functional diversity [8,9]. Soil microbial community structure and composition can reflect the response of soil to vegetation restoration, so it is necessary to study the microbial changes in the process of vegetation restoration [10]. DOM provides soluble organic substrates to support and sustain the growth and activity of soil microbial communities [11], while microorganisms also have the ability to decompose and use, as well as synthesize, DOM molecules [12], but less is known about the specific link between the two. Therefore, understanding the interactions between soil microbial communities and DOM molecules is essential for predicting the dynamics of soil carbon after restoration [13,14].

In this paper, soils from different vegetation restoration stages were collected in a subtropical red soil erosion area (Changting, Fujian). The chemical diversity of soil DOM during vegetation restoration was investigated by Fourier-transform ion cyclotron resonance mass spectrometry (FT-ICR MS), and the changes of bacteria and fungi during vegetation restoration were investigated by high-throughput sequencing. We hypothesized that (1) the chemical diversity of soil DOM and the richness of microbial community would increase with the recovery time series and (2) that soil nutrients would affect soil microbial community, which is closely related to soil DOM molecules. By analyzing the possible complex relationships between soil DOM molecules, bacteria, and fungi, the interaction between soil microbial community and DOM chemical diversity was elucidated, in order to provide a basis for soil health evaluation and scientific management of soil erosion area ecosystem, as well as for the study of the global carbon cycle.

2. Materials and Methods

2.1. Study Area and Sample Collection

The study was conducted at the Changting restoration site, located between 25°18′40″–26°2′5″ N and 116°0′45″–116°39′20″ E, in the western part of Fujian Province in southeastern China. It has a typical subtropical monsoon climate. The annual average temperature is 18.1 °C, the annual average rainfall is 1710 mm, the annual average evaporation is 1403 mm, the frost-free period is 260 days, and the year-round sunshine duration is 1925 h [15]. The main soil type is red soil (according to the Chinese Soil Taxonomy (CST) system, which roughly corresponds to Ultisols, Oxisols, and certain Alfisols, as recognized by the USDA Soil Taxonomy system) [16], aluminum, iron-rich, and developed on a granite parent material. Although deep, the soil structure is loose, and the evergreen broadleaf forest cover has been severely degraded by human disturbance, leading to increased soil erosion. Since the 1940s, large-scale vegetation restoration and erosion control treatment projects have been carried out in the Changting area through direct seeding of mainly *Pinus massoniana* Lamb., creating artificial forests with different types.

According to the general process of forest succession, five sites of different ages and similar conditions were selected for this research. These sites were untreated bare land (BL) (as the control), newly restored young coniferous forest (YC), slightly more mature coniferous forest (MC), mixed coniferous and broadleaf forest (CB), and broad-leaved forest (BF). Before the revegetation, the soil was eroded and the A horizon was stripped out, while the B horizon was only 5–10 cm. The restoration was implemented mainly by direct seeding of *Pinus massoniana* Lamb., with later planting of some broadleaved species. The BL comprised shallow gullies on bare bedrock and had severe slope erosion and sparse

vegetation. Some bedrock at the top of the slope was exposed, and the litter depth was minimal. The YC (6 year-old restoration site) was mostly covered with vegetation; the main vegetation was *Dicranopteris dichotoma* (Thunb.) Bernh. and *Pinus massoniana* Lamb. The MC (13 year-old restoration site) had a depth of 0–3 cm of litter and the dominant vegetation was *Dicranopteris dichotoma* (Thunb.) Bernh., *Pinus massoniana* Lamb. and *Lespedeza bicolor* Turcz. The litter thickness was 3–8 cm in the CB and was dominated by the growth of *Dicranopteris dichotoma* (Thunb.) Bernh., *Schima superba* Gardn. et Champ, *Ilex pubescens* Hook. et Arn. In BF, a shrub layer had developed under the forest cover; the soil humus layer was deep and litter thickness was 3–10 cm. The sample site is dominated by *Schima superba* Gardn. et Champ, *Liquidambar formosan* Hance, and some *Pinus massoniana* Lamb. In July 2018, we set up three replicate plots (20 × 20 m) in each restoration site. In each plot, soils at 0–20 cm depth were collected at 6 points with a soil drill according to the S-shaped sampling design and combined to form composite soil samples in each replicate plot. The soil samples were immediately transported to the laboratory in a cool box.

2.2. Analysis of Soil Chemical Properties

Part of the collected soil samples was stored in an ultra-low temperature freezer ($-80\ °C$) for later analysis for DOM, microorganisms, and other indicators, while the remainder were air-dried for about a week. Pure water without CO_2 was added to the air-dried soil (solid to liquid ratio 1:2.5) and allowed to stand for 30 min; then, the soil pH was measured using a pH probe and meter (ST3100-F (Ohaus, NJ, USA)) [17]. The concentrations of available nitrate (NO_3^-) and ammonium (NH_4^+) were determined by a continuous flow analyzer (SAN^{++}, Skalar, Netherlands) after extracting fresh soil with $2\ mol·L^{-1}$ KCl solution at a solid to liquid ratio of 1:10 after stirring for 10 min, centrifuging for 10 min at $2800×\ g$, and filtering the supernatant with a qualitative filter paper [18]. The same extraction procedure was used for measuring soil dissolved organic carbon (DOC) content, apart from filtering the supernatant with a 0.45 μm polyethersulfone (PES) filter [19], before analysis using a total organic carbon analyzer (TOC-L CPH Analyzer, Shimadzu, Japan). Total carbon (TC) and total nitrogen (TN) content were determined on 0.75 g air-dried soil samples (sieved to 100 μm) by dry combustion in a Carbon Nitrogen Analyzer (Vario MAX, Elementar, Germany) [8].

2.3. Molecular Analysis of Soil DOM

Dissolved organic matter (DOM) in soil samples from different restoration ages was extracted for molecular analysis by solid phase extraction. Three samples from each site were mixed in equal proportions into one composite soil sample. Briefly, 12 g of fresh soil stored at $-80\ °C$ was placed in a 100 mL centrifuge tube with 60 mL of water (18 MΩ) (1:5 solid to liquid ratio) and then centrifuged for 8 h in a constant temperature shaker ($25\ °C$, 170 rpm) [20]. The filtered (0.45 μm) supernatant was flushed with pure methanol (mass spectrometry grade) in an activated SPE box (Bond Elut PPL, 500 mg, 6 mL, Agilent Technology, Santa Clara, CA, USA), and then acidified in a filter cartridge with acidified Milli-Q water (pH = 2). After completely drying the cartridge with high-purity N_2 gas, DOM was eluted from the cartridge with methanol (5 mL), with a final concentration of about $20\ mg\ L^{-1}$ [21]. The molecular composition of soil samples was further analyzed by FT-ICR MS and 9.4T superconducting magnets (Bruker Apex Ultra, Bruker, Germany). Negative ions were typically formed at a spray shielding voltage of 4 kV, a capillary column voltage of 4.5 kV, and a capillary end voltage of 320 V. The quality range was set at 200–800 *m*/*z* [22]. More details of the FT-ICR MS methods and data analysis are provided in Supplementary Materials Section S1.

2.4. Analysis of Soil Microbial Community

Soil bacterial and fungal communities were determined using 16S and ITS1 rDNA gene Illumina sequencing, respectively. DNA was extracted from 0.25 g soil using a DNA kit (Omega Bio-Tek, Norcross, Georgia, USA) and then stored at $-20\ °C$ for subsequent

analysis. After genomic DNA was extracted from the samples, the 16S rDNA of soil bacteria was amplified, targeting the V3 + V4 region. The primer sequences were 338F (5′-ACTCCTACGGGAGGCAGCAG-3′) and 806R(5′-GGACTACNNGGG TATCTAAT-3′) [23]. Amplification of the internal transcribed spacer (ITS) region of fungal ribosomal DNA was achieved by using primers ITS1 (5′-CTTGGTCATTTAGAGGAAGTAA-3′) and ITS2 (5′-TGCGTTCTTCATCGATGC-3′). The PCR reaction system comprised 12.5 μL, 2 × Taq PCR mastermix, 3 μL BSA (2 ng μL^{-1}), 2 primers (5 μM), 2 μL template DNA, and 5.5 μL double-distilled water. The reaction parameters were pre-denaturation at 95 °C for 5 min, denaturation at 95 °C for 45 s, annealing at 55 °C for 50 s, elongation at 72 °C for 45 s, 32 cycles, and elongation at 72 °C for 10 min. Amplification products were detected by 2% agarose gel electrophoresis and paired sequencing was performed on an Illumina HiSeq 2500 platform at Allwegene Technologies (Beijing, China) to determine the microbial community structure of the samples. The microbial sequencing data were obtained from Hu et al. (2021) [24].

2.5. Data Analysis

Following the determination of DOM by FT-ICR MS, compound groups were distinguished according to their elemental ratios, double bond equivalence (DBE), H/C, and O/C. Furthermore, the DOM formulae (Table S1) were visualized in van Krevelen diagrams and classified into six distinct biochemical classes [25]. DBE, H/C, O/C, the mass-to-charge ratio (*m*/*z*), the average nominal oxidation state of carbon (NOSC), the Shannon index, and the Pielou index were calculated (see Section S2 for details). The α-diversity measurements of soil bacteria and fungi, including Chao1 richness and Shannon's diversity index, were calculated for each site [22]. Data were tested for normality by the Shapiro–Wilk test, and single factor ANOVA was performed to determine significant differences in Chao1 richness and Shannon's diversity index among restoration sites of different types, followed by least significant difference (LSD) tests or Tamhane's T2 test. The importance and significance of soil environmental factors on microbial alpha diversity were assessed on the R platform using the random forest of the "rfPermute" package and ranked, and the significance of the full model was assessed using the "A3" package [26]. After removing collinearity, redundancy analysis (RDA) was performed on the R platform for soil bacterial genera and fungal genera with relative abundances greater than 1%. The specific links between DOM chemodiversity and soil microbial community were revealed by network analysis. Pearson correlations (*p* < 0.01) were calculated to determine the associations between individual DOM molecules and microbial community operational taxonomic units (OTUs). DOM molecules and OTUs with significant correlations were drawn in network analysis figures using Cytoscape v.3.5.1. The correlation values were prioritized based on their size to reduce network complexity and identify key linkages. A Mantel test and a heat map of the correlations were conducted using the Tutools platform (https://www.cloudtutu.com/) (accessed on 10 September 2022). Unless otherwise stated, SPSS v.19 was used for all statistical analyses, with a significance level of *p* < 0.05.

3. Results

3.1. Characterization of DOM Chemodiversity

The major classes of compounds in soil DOM were lipids, aliphatic/proteins, lignin/carboxylic rich alicyclic molecules (CRAM)-like structures, carbohydrates, unsaturated hydrocarbons, aromatic structures, and tannins (defined in Table S1), while the subcategories included CHO, CHON, and CHOS. The van Krevelen diagrams in Figure 1a–e show that the CHO subcategory was distributed between lipids, aliphatic/proteins, lignin/CRAM-like structures, carbohydrates, aromatic structures, and tannins. The CHON subcategory occurred mainly as aliphatic/proteins, lignin CRAM-like structures, and tannin regions, while the CHOS subcategory was more concentrated in high H/C and high O/C regions. The relative proportion of CHO, CHON, and CHOS compounds differed among sites (Figure 1f). CHO compounds were the dominant DOM major subcategories at all sites,

with the proportion increasing with restoration age. The relative abundance of CHON compounds in YC was slightly higher than that in BL (as control), then relative abundances of MC and CB decreased, before increasing again in BF. The CHOS content showed an overall downward trend with increasing restoration age. The relative abundance of major compound classes varied among sites (Figure 1g). The largest proportion of soil DOM was derived from lignin/CRAM-like structures. Both lipids and aliphatic/proteins had a downward trend with increasing restoration age, especially lipids, which almost disappeared in the sites MC, CB, and MF.
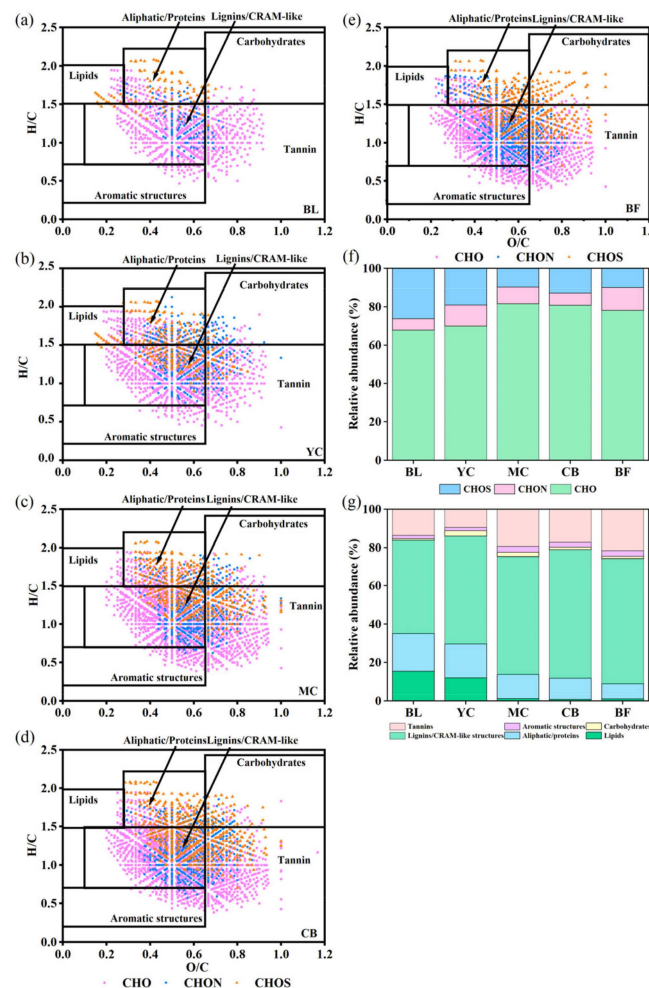

Figure 1. Van Krevelen diagrams of CHO, CHON, and CHOS subcategories in dissolved organic matter (DOM) from soils along a vegetation restoration chronosequence for bare land (BL) (**a**), newly restored young coniferous forests (YCs) (**b**), slightly more mature coniferous forests (MCs) (**c**), mixed coniferous and broadleaf forests (CBs) (**d**) and broad-leaved forests (BFs) (**e**). The black lines in the van Krevelen diagrams correspond to major classes of compounds that can be expected in DOM. Bar diagrams show the contribution of the (**f**) major subcategories and (**g**) major classes in each site. CHO: DOM molecules containing carbon, hydrogen, and oxygen atoms; CHON: DOM molecules containing carbon, hydrogen, oxygen, and nitrogen atoms; CHOS: DOM molecules containing carbon, hydrogen, oxygen, and sulfur atoms.

The DOM molecules that disappeared following restoration were mainly located in the higher H/C region, especially in the lipid region (Figure 2). The resistant DOM molecules were distributed between aliphatic/proteins, lignin/CRAM-like structures, carbohydrates, aromatic structures, and tannins. DOM molecules with lignin/CRAM-like structures were produced throughout vegetation restoration (Figure 2a–d). In the early stage of vegetation restoration, predominantly aliphatic/proteins and carbohydrates were

produced (Figure 2a), while more tannins and lignin/CRAM-like structures were produced later in vegetation restoration (Figure 2c,d).
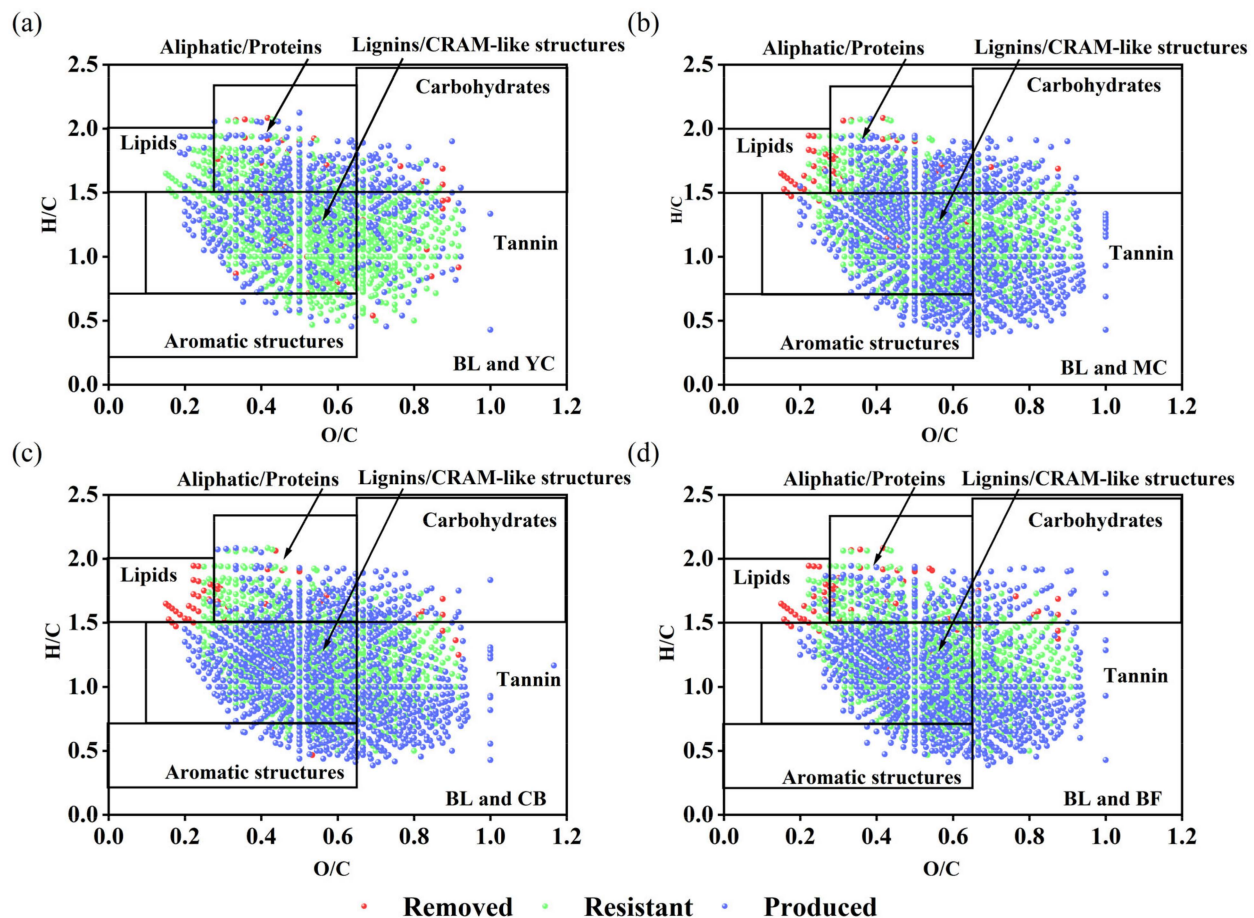

Figure 2. Van Krevelen diagrams of soil dissolved organic matter (DOM) comparisons between the BL (as control) and YC (**a**), MC (**b**), CB (**c**), and BF (**d**). Points in red represent DOM molecules that disappeared after vegetation restoration (removed), points in green represent DOM molecules that were unchanged (resistant), and points in blue denote new molecules that appeared during vegetation restoration (produced). BL: bare land; YC: newly restored young coniferous forest; MC: slightly more mature coniferous forest; CB: mixed coniferous and broadleaf forest; BF: broad-leaved forest.

The mean molecular weight of samples ranged from 356.90 to 400.38, increasing after vegetation restoration, and stabilizing as the vegetation was restored to slightly mature coniferous forest (Table 1). The average O/C value of DOM increased slightly while the average H/C value decreased over the vegetation restoration chronosequence. The DBE increased from 6.82 to 8.19, and the Shannon index, the Pielou index, and the NOSC of DOM molecules also increased compared with BL, which corresponded to the decrease in H/C value. The percentage of DOM molecules with H/C < 1.5 (lignin/CRAM-like structures, aromatic structures, and tannins) increased with chronosequence age, while the percentage of DOM molecules with H/C > 1.5 (aliphatic/proteins, carbohydrates, and lipids) decreased. Molecular weights of DOM across soil samples from all sites ranged from 157 m/z to 640 m/z (Figure 3a). The peak molecular weight of DOM in soil shifted from 300 to 350 following revegetation. The m/z peak percentage of soil DOM decreased from 39% in bare land to 33% in young coniferous forests and finally to 27% in broadleaf forests, indicating increased soil DOM diversity and complexity after restoration. The relative abundances of peak carbon mass distribution decreased along the chronosequence of vegetation restoration (Figure 3b).

Table 1. Characteristics of soil dissolved organic matter (DOM) in five plots of different forest types, BL, YC, MC, CB, and BF, after vegetation restoration, such as the intensity-weighted average of the molecular composition of soil samples, double bond equivalent (DBE), hydrogen/carbon (H/C), oxygen/carbon (O/C), the Shannon index, Pielou's evenness index, the NOSC (average nominal oxidation state of carbon), DOM molecules with H/C > 1.5, and DOM molecules with H/C < 1.5. BL: bare land; YC: newly restored young coniferous forest; MC: slightly more mature coniferous forest; CB: mixed coniferous and broadleaf forest; BF: broad-leaved forest.

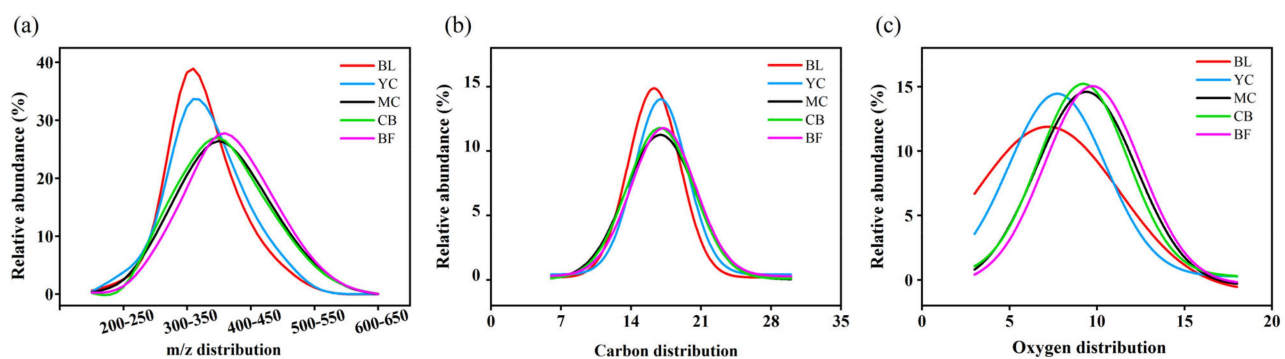| Site	DBE	H/C	O/C	*m/z*	Shannon Index	Pielou Index	NOSC	H/C > 1.5	H/C < 1.5
BL	6.82	1.23	0.54	356.90	6.18	0.88	−0.11	35.81%	64.19%
YC	6.56	1.29	0.53	369.20	6.85	0.91	−0.16	32.43%	67.57%
MC	7.70	1.20	0.57	395.20	7.31	0.93	0.02	16.17%	83.83%
CB	8.00	1.18	0.56	400.38	7.21	0.91	0.01	13.26%	86.74%
BF	8.19	1.16	0.57	399.34	7.28	0.93	0.06	10.20%	89.80%

Figure 3. Characteristics of dissolved organic matter molecules in soil samples from sites of different forest types, BL, YC, MC, CB, and BF. The distribution of the mass-to-charge ratio (*m/z*) (**a**), the distribution of Cx class species (**b**), and the distribution of Ox class species (**c**). BL: bare land; YC: newly restored young coniferous forest; MC: slightly more mature coniferous forest; CB: mixed coniferous and broadleaf forest; BF: broad-leaved forest.

3.2. Characterization of the Microbial Community

The clustering analysis was carried out at a 97% similarity level to produce a Venn diagram of bacterial and fungal OTUs. The number of soil bacterial OTUs generally increased with time since restoration, with 1042, 1331, 1316, 1340, and 1536 OTUs at sites BL, YC, MC, CB, and BF, respectively; for a total of 2145 OTUs (Figure S3a). A total of 491 bacterial OTUs were found across sites of all types, indicating a high degree of similarity in soil bacterial composition between sites. The number of soil fungal OTUs also broadly increased along the chronosequence, with 784, 453, 993, 1207, and 1265 OTUs at sites BL, YC, MC, CB, and BF, respectively; for a total of 4702 OTUs (Figure S3b). The total number of fungal OTUs common to all sites was 145, indicating that the soil fungal composition varied considerably between sites and that the fungal community changed significantly with the recovery of vegetation.

Vegetation restoration had significant effects on the diversity of soil bacterial and fungal communities (Figure 4). With the restoration of vegetation, the diversity (Shannon) and richness (Chao 1) of bacteria showed an increasing trend. Of all the indicators, the magnitude of change in bacterial richness was the largest and most significant. The trend of fungal diversity was similar to that of soil bacteria, with a significant increase in fungal diversity at the MC, CB, and MF sites, but little difference between the BL and YC sites. Soil bacterial and fungal alpha diversity indices showed little change in the later stages of revegetation, indicating that soil bacterial and fungal diversity gradually stabilizes with revegetation.
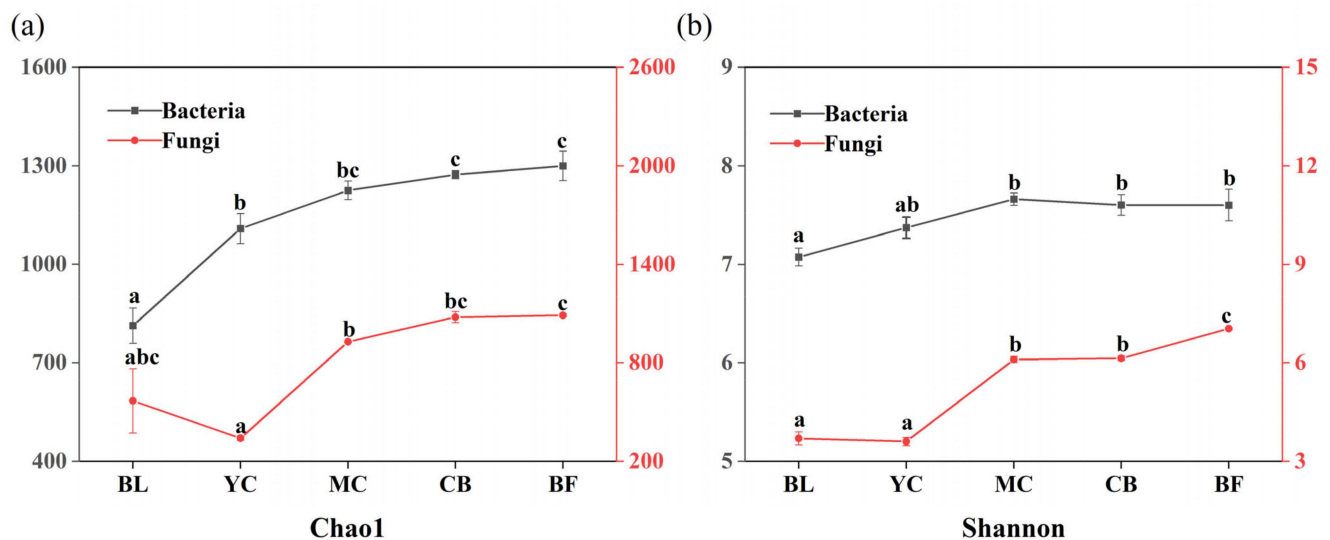
(a)

(b)

Figure 4. Soil bacterial and fungal alpha diversity measurements in sites YC, MC, CB, and BF compared to control sites (BL). The black line and the axes indicate the alpha diversity of the bacterial community, while the red line and the axes indicate the alpha diversity of the fungi. Values are means ± SE (n = 3). Different letters above the datapoints indicate significant differences ($p < 0.05$) in bacterial/fungal diversity measures among sites according to the least significant difference (LSD) test or Tamhane's T2 test. The alpha diversity measures of Chao 1 (richness) (**a**) and Shannon (diversity) (**b**) in soils from sites of different forest types. BL: bare land; YC: newly restored young coniferous forest; MC: slightly more mature coniferous forest; CB: mixed coniferous and broadleaf forest; BF: broad-leaved forest.

3.3. Characterizing the Relationship between Soil Microbial Communities, DOM Molecular Composition, and Soil Properties

Forest restoration is accompanied by increased soil nutrient concentrations (Figure S1). The concentrations of TC, DOC, and TN in soil increased with the restoration of vegetation. The relationship between soil environmental factors and soil microbial community alpha diversity was analyzed by random forest (Figure 5a–d). Compared with other environmental factors, TC, DOC, and NH_4^+ had higher MSE%, indicating that TC, DOC, and NH_4^+ are important environmental elements affecting soil bacterial and fungal diversity. In comparison, pH has a higher important value for bacteria Chao1, while TC and DOC had a higher importance value for fungi. To determine the relationship between specific microbial species and soil chemistry, we performed redundant analyses of bacterial genera and fungal genera with relative abundances greater than 1%. Redundancy analysis showed that soil TN, DOC, NH_4^+, and NO_3^- concentrations and pH were significantly correlated with various bacterial genera (Figure 5e and Figure S4b). *Burkholderia-Paraburkholderia* was negatively correlated with TN, while *Acidothermus* and *Acidibacter* were positively correlated with TN, DOC, and NH_4^+ and negatively correlated with pH. *Archaeorhizomyces* was positively correlated with soil pH and negatively correlated with DOC, NH_4^+, and TN (Figure 5f). Conversely, *Russula* was positively correlated with TN, NH_4^+, DOC, and NO_3^- and negatively correlated with pH.
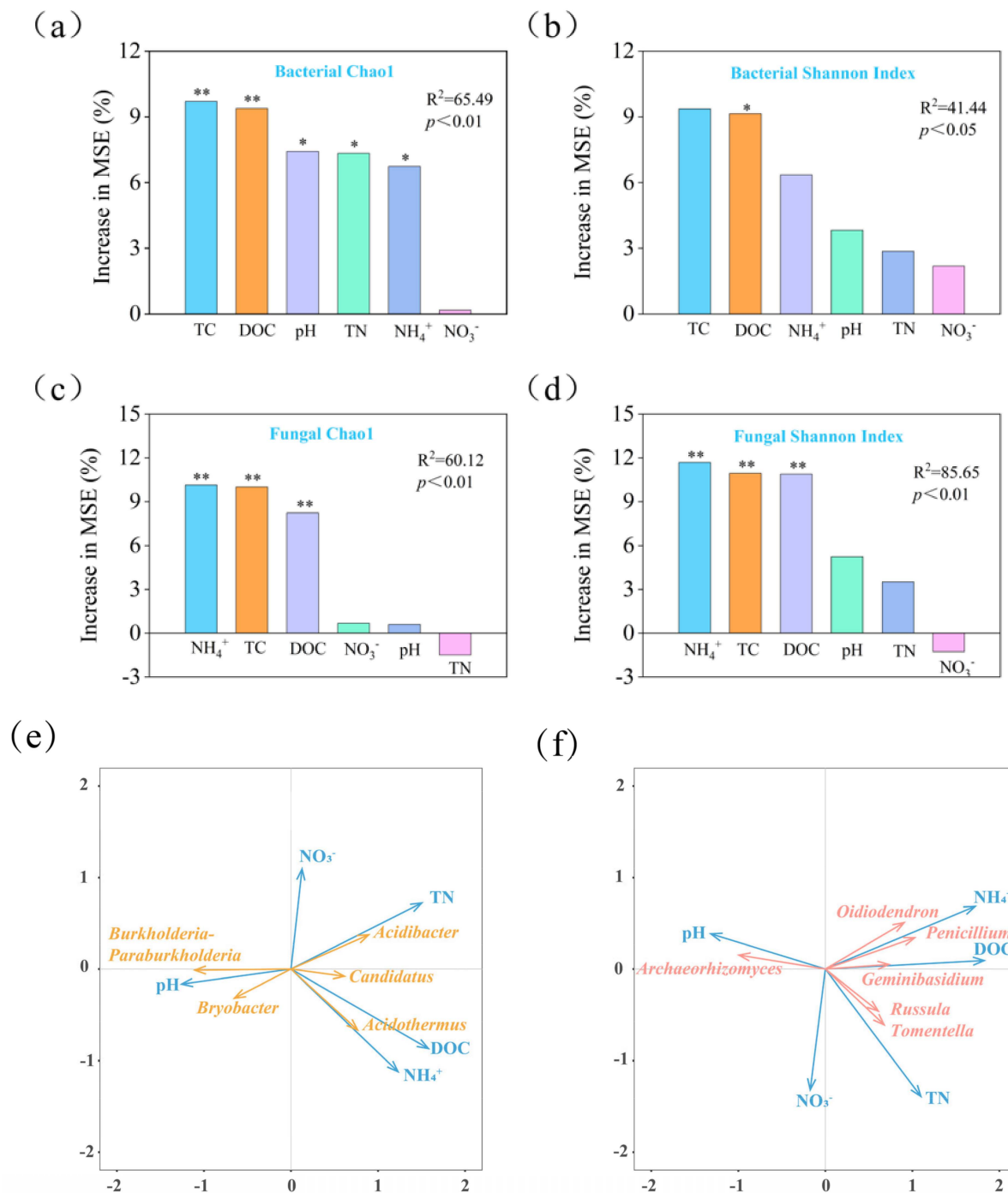
Figure 5. Random forest plot between soil environmental factors (TC, DOC, pH, TN, NH_4^+, and NO_3^-) and soil microbial alpha diversity (Chao1 and Shannon index), indicating the importance (percentage of increase in the mean squared error) of soil environmental factors for Chao1 bacteria (**a**), Shannon index bacteria (**b**), Chao1 fungi (**c**) and Shannon index fungi (**d**). Significance levels are * $p < 0.05$ and ** $p < 0.01$. MSE, mean squared error. Redundancy analysis ordination maps based on the relative abundance of soil bacterial genus (**e**) and fungal genus (**f**) exceeding 1%. Bacteria (orange arrows) and fungi (pink arrows) and environmental variables (blue arrows). TN: total nitrogen; TC: total carbon; DOC: dissolved organic carbon; NO_3^-: nitrate nitrogen; NH_4^+: ammoniacal-nitrogen; pH: the potential of hydrogen.

A co-occurrence network analysis to identify the interconnections between the chemodiversity of soil DOM and soil microbial community showed differential links between DOM

molecules and soil microbes (Figure 6). For the top 100 bacterial OTUs with the highest relative abundance and the top 100 most abundant DOM molecules in soil samples from the five sites, there were 370 significant correlations, 41 of which linked 27 DOM molecules to 22 OTUs ($p < 0.01$) (Figure 6a). At the phylum taxonomic level, these 22 OTUs comprised *Proteobacteria* (8), *Acidobacteria* (7), *Chloroflexi* (5), *Actinobacteria* (1), and *Firmicutes* (1). *Acidobacteria* and *Proteobacteria* had the highest number of significant OTUs. There was a positive correlation between *Acidobacteria* and DOM molecules, whereas *Proteobacteria* exhibited mostly positive correlations with DOM molecules and some negative correlations. In contrast, *Chloroflexi* was mostly negatively correlated with DOM molecules (Figure 6a). Thirty eight significant correlations were identified between the top 50 highest relative abundance fungal OTUs and the top 100 most abundant DOM molecules, with 28 linking 26 DOM molecules to 18 OTUs ($p < 0.01$) (Figure 6b). These OTUs comprised *Ascomycota* (eleven OTUs) and *Basidiomycota* (seven OTUs). While *Basidiomycota* showed a significant positive correlation with DOM molecules, *Ascomycota* displayed mainly a negative correlation with DOM molecules and some positive correlations with a few DOM molecules (Figure 6b).
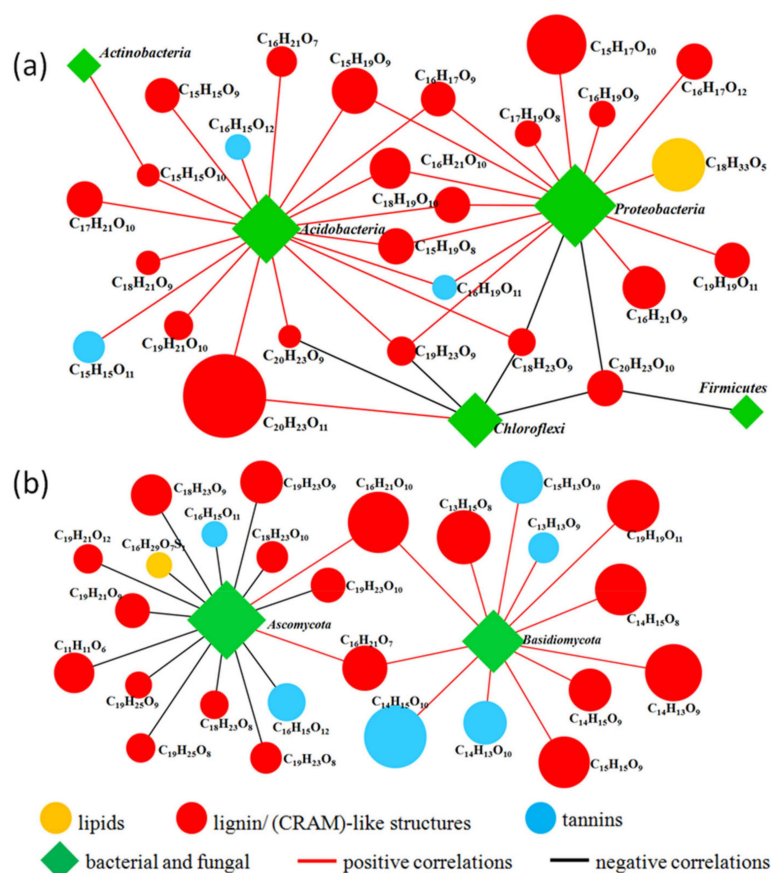

Figure 6. Interaction network analysis of the top 100 most abundant bacterial operational taxonomic units (OTUs) (**a**), top 50 most abundant fungal OTUs (**b**), and top 100 most abundant dissolved organic matter molecules in soil samples from the five sites of different forest types with significant correlations ($p < 0.01$). Red circles are lignin/carboxylic rich alicyclic molecule (CRAM)-like structures, blue circles are tannins, and yellow circles are lipids; rhombuses are bacterial and fungal OTUs (green). Dissolved organic matter molecules' relative abundances are proportional to node size. Red lines indicate positive correlations and black lines indicate negative correlations.

In order to show the relationship between the microbial community and soil chemical properties and soil DOM categories, a Mantel test was performed (Figure 7a). Microbial communities had significant positive correlations with most of the soil chemical properties and soil DOM categories ($p < 0.01$; r ≥ 0.4). Bacterial and fungal communities were

significantly positively correlated with AK, NH_4^+, TC, and DOC. The correlation between bacterial communities ($p < 0.01$; r $\geq$ 0.4) and carbohydrates was stronger than that of fungal communities ($0.01 \leq p < 0.05$, $0.2 \leq$ r < 0.4). The heat map (Figure 7b) between soil microbial diversity and soil DOM showed a significant positive correlation between the soil DOM Shannon index, the Pielou index, and bacterial diversity, while NOSC showed a significant positive correlation with soil fungal diversity.
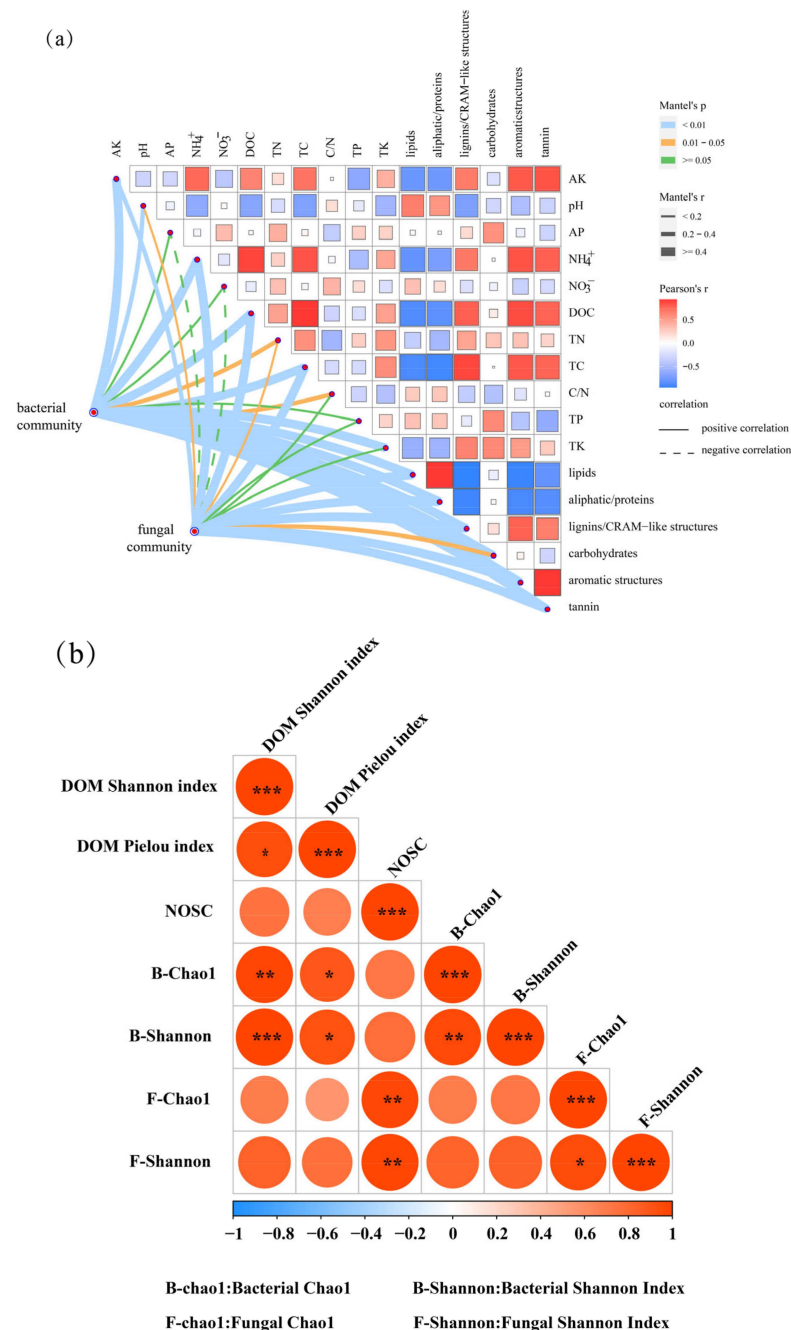

Figure 7. Mantel test between soil chemistry, soil dissolved organic matter, and soil microbial communities (bacterial and fungal communities) (**a**) AP: available phosphorus; AK: available potassium; DOC: dissolved organic carbon; TC: total carbon; TN: total nitrogen; TP: total phosphorus; TK: total potassium; C/N: ratio of total carbon to total nitrogen; NO_3^-: nitrate nitrogen; NH_4^+: ammoniacal-nitrogen; pH: the potential of hydrogen. Heat map of correlations between dissolved organic matter general characteristics and soil microorganisms (bacteria and fungi) (**b**) Significance levels are * $0.01 < p < 0.05$, ** $0.001 < p < 0.01$, and *** $p \leq 0.001$.

4. Discussion

4.1. DOM Molecules Become More Complex and Difficult to Degrade with Restoration Age

Soil DOM is dominated by lignin/CRAM-like structures, whereas lipids and aliphatic/proteins decreased with increasing restoration age. One reason for these trends may be due to changes in the intrinsic characteristics of DOM over time, with the DOM molecules produced at the start of restoration being unstable and easy to decompose, and the increasing dominance over time of more stable DOM molecules that are more resistant to decomposition [27]. An alternative, and possibly simultaneous process, is changes in preferences of organic matter utilization of the soil microbial community as it develops after restoration, resulting in changing degrees of decomposition and transformation of different DOM molecules [28]. Supporting these observed trends, the DOM molecules that disappeared following restoration were mainly located in the higher H/C region, especially in the lipids region, whereas more tannins and lignin/CRAM-like structures were produced later in vegetation restoration (Figure 2). The soil DOM molecular composition at the restored sites tended to have lower H/C and wider O/C ratios compared to the control, indicating increasing soil DOM recalcitrance with time after restoration [29] since DOM molecules with a high O/C ratio and low H/C ratio are more biodegradable [30].

The increase in the peak molecular weight of DOM in soil indicates an increase in the molecular weight of the newly formed substances and the polymerization of DOM molecules [31]. The average molecular weight of the samples, O/C, DBE, NOSC, the Shannon index, and Pielou's evenness index, generally increased along the chronosequence, indicating that the diversity and uniformity of soil DOM molecules increased after vegetation restoration, and DOM molecules tended to become more recalcitrant and complex [29], which may be due to the differential preferences of soil microorganisms for decomposing and utilizing organic matter [32]. Li et al. (2018) concluded that DOM molecules with H/C > 1.5 are readily degradable, while DOM molecules with H/C < 1.5 are difficult to degrade [21]. The proportion of recalcitrant DOM molecules in this study increased with revegetation, indicating that revegetation is beneficial to soil carbon sequestration. The changing shape of the distribution curve of DOM molecular masses indicates that the conversion rate of organic matter decreased and the stability and persistence of DOM molecules increased after vegetation restoration. This increasing diversity in the composition of produced DOM may be due to the complexity of vegetation cover and increased soil microbial diversity along the restoration chronosequence [28]. It has been proposed that DOM has high chemodiversity, with individual compounds present in only low concentrations, thus limiting the encounter rate of the same molecule with microbes and preventing microbial degradation [33]. Therefore, the recalcitrance of DOM is expected to increase with time since restoration, as supported by the decrease in peak relative abundance of carbon mass distribution along the chronosequence. Additionally, the majority of DOM molecules produced had a high C content (carbon number > 19) and high DBE values (>7) (Figure S2), evidence of the molecular stability of DOM [27]. The rate of formation of oxygen-containing substances slowed down over time after vegetation restoration, indicating that the conversion rate of organic matter decreased while the persistence of newly generated DOM increased [21], as also confirmed by the DOM mass distribution and carbon distribution curves.

These results indicate that DOM compounds of low DBE value with low aromatic and high alkyl structures are less stable and more likely to undergo transformation to produce more persistent organic matter with a high carbon number and high DBE values [22,34]. Compared with the bare land, except for the newly restored coniferous forest, which produced less new DOM, the other sites produced more new DOM. It may be that the recovery time of the nascent coniferous forest is too short to increase soil fertility to support the substantial production of new DOM. It is also possible that the young forest has not reached canopy closure, thus leaving the soil unprotected from rain events [35]. The smaller amount of produced DOM in soils from BF compared with the CB may be accounted for by the observation that soil carbon tends to be stable and not readily transformed during

vegetation restoration. The concentration, composition, and properties of soil DOM in areas of vegetation restoration depend on the sources and transformation processes. DOM has been shown to be mainly released from the decomposition of deciduous leaf litter, deadwood, plant root exudates, microbial primary and secondary metabolites, and degradation products of soil organic matter [28,36]. DOM is described as a continuum with labile, semi-labile, and refractory pools that are decomposed and utilized by microorganisms on time scales from minutes to millennia [28]. Molecular analysis of terrigenous DOM revealed that the less oxygenated molecules were more biodegradable [37]. This is consistent with our finding that during revegetation, the removed DOM molecules have a lower oxygen number, while the produced DOM molecules have a higher oxygen number and are less susceptible to biodegradation.

4.2. Different Changes of Soil Bacteria and Fungi during Vegetation Restoration

Soil bacterial and fungal alpha diversity indices gradually stabilized as the vegetation recovered, with more pronounced changes in soil bacterial richness, indicating that soil nutrients were the main factor influencing soil bacteria. The marked increase in soil fungal richness in the MC, CB, and MF sites (vegetation restoration time greater than 6 years) was most likely due to new habitat niches created by new plant species, indicating that plant richness was the main control of soil fungi. Another important control may be that fungi mainly decompose and utilize root cortex and leaves and branches with more cellulose [38–40]. Fungi obtain nutrients predominantly from decomposing vegetation and also prefer cellulose-rich substrates that will accumulate later during vegetation succession [8]; thus, the fungal diversity in restored sites with young coniferous forests changed little compared with bare land. The observed patterns of microbial diversity may be related to the increased soil nutrient content during vegetation restoration (Figure S1), as also observed in previous studies [8,41]. Soil microorganisms remain key regulators in biogeochemical cycling and transform non-available nutrient elements into available forms, thus increasing the soil nutrient content [42]. Correspondingly, soil nutrients were utilized by microorganisms, and soil nutrient content affected the microbial community [43]. Therefore, vegetation restoration improved soil nutrient content and microbial diversity as a whole. The observed delay in increased fungal diversity compared to bacterial diversity after vegetation restoration can be attributed to different nutrient acquisition mechanisms, with bacteria mainly responding to soil nutrients and plant root exudates, while fungi obtain nutrients predominantly from decomposing vegetation that does not accumulate substantially until later in the chronosequence [8,43].

4.3. Linkages between Soil Microbial Communities, DOM Molecular Compositions, and Soil Properties

The increased soil TC, DOC, and TN can be related to the accumulation of tree litter inputs over time that decompose relatively quickly as the intrinsic microbial community adapts to this new substrate. The change in soil carbon content may be related to the change in forest type. It has been found that when *Schima superba* is mixed with *Pinus massoniana* the soil carbon content increases significantly [44]. Changes in vegetation type are accompanied by changes in plant diversity, biomass production, and the biochemical composition of litter [45]. Changes in the quality and quantity of organic matter can significantly affect the structure and composition of the main decomposers (fungal communities) in the soil, which explains the higher important of TC and DOC for fungi. It could also be related to the minimal decomposition of the intrinsic soil organic carbon by microorganisms, thus resulting in a delay in C mineralization after reforestation. Previous studies have reported that soil carbon sequestration rate and soil organic C content increase during vegetation succession in tropical montane cloud forest areas and adjacent degraded open grazing land [46], which is consistent with our results. The soil TN content is notably high in YC, which might be due to increased vegetation cover causing microorganisms to produce more N-containing organic matter [47], as well as early colonization by nitrogen-fixing

plants. The high TN content in BF could be attributed to the abundance of soil microbial communities that facilitate the decomposition of more N-rich litter.

Acidothermus and *Acidibacter* are important bacterial genera of *Acidobacteria*, which live in acidic soil environments [48], and thus their abundances were negatively correlated with soil pH. Chen et al. (2021) found that the relative abundance of *Acidothermus* was positively correlated with soil NH_4^+ concentration [49]. After vegetation restoration, changes in soil chemical properties mediate bacterial composition and association. A positive correlation was found between the relative abundance of *Ascomycota* and soil pH, whereas a negative correlation was found with DOC, NH_4^+, and TN (Figure S4c). Since *Archaeorhizomyces* is an important genus in *Ascomycota*, their associations with soil properties during vegetation restoration are the same. *Basidiomycota* is a K-strategist that is suitable for growth in fertile soils [50] and is positively correlated with DOC, NH_4^+, TN, and NO_3^- (Figure S4c). *Basidiomycota* can decompose forest litter and combine with other mycorrhizal fungi, so its relative abundance increases with vegetation restoration, and it is positively correlated with soil DOC concentrations [51]. *Russula* mostly belongs to *Basidiomycota* [50], thus showing the same environmental preference as *Basidiomycota*. Our results show that vegetation restoration plays an important role in changing soil chemical properties, which in turn impacts the structure and composition of soil microbial communities.

DOM molecules related to bacteria mainly belonged to lignin/CRAM-like structures, and a few were tannins, indicating that lignin/CRAM-like structures and tannins were more stable in soil from sites at different vegetation restoration stages. Compared to lipids and aliphatic/proteins, lignin/CRAM-like structures contain more aromatic rings and have higher oxidation states, making them more resistant to degradation by bacteria [52]. Previous research indicates that specific bacteria can produce or degrade only specific DOM molecules, and changes in DOM occur at different rates [53], and some of these DOM substances may be intermediates for microbial decomposition and synthesis. For example, *Actinobacteria* can catalyze oxidation reactions and *Proteobacteria* is highly effective at degrading organic matter [37]. In this study, DOM molecules related to fungi were mainly lignin/CRAM-like structures, a few were tannins, and one was an aliphatic/protein, indicating that lignin/CRAM-like structures and tannins always existed and were resistant to fungal decomposition during vegetation restoration. Within the *Basidiomycota* phylum of soil fungi, an important order is the *Agaricales*, which can decompose lignins and other substances by mycorrhizal associations and with other *Basidiomycota* fungi [8]. The lower temperatures in spring and winter in the study area (10.4–27.4 °C and 4.5–16.5 °C, respectively) may suppress microbial activities, resulting in the accumulation of a large amount of readily biodegradable DOM [54]. During higher temperatures in summer (21.9–33 °C), microorganisms preferentially use degradable DOM, making residual DOM molecules more recalcitrant, such as lignin/CRAM-like structures [55]. The significant positive correlations between specific fungal taxa and specific DOM molecules in this study indicated fungal specialization on particular DOM molecules. Lipids and aliphatic/proteins were shown to be easily degradable and related to microbial activity, with increased microbial abundance accelerating the degradation of lipids and aliphatic/proteins [56]. Therefore, with increasing time of vegetation restoration the lipid and aliphatic/protein content of soil DOM decreased. Lignin/CRAM-like structures are highly diverse and bioresistant due to the substantial content of alicyclic rings and branching [37].

Bacterial and fungal communities were significantly positively correlated with AK, NH_4^+, TC, and DOC, indicating that these environmental variables play an important role in the construction and composition of microbial communities [57,58]. Bacteria have the ability to utilize and decompose carbohydrates, especially at high temperatures, and the decomposition efficiency is increased [59], so the correlation between bacterial communities and carbohydrates is stronger than that between fungal communities. The microbial community was mostly positively correlated with DOM molecules, but there were positive and negative correlations in the co-occurrence network analysis, which further confirmed the specialization of DOM biodegradation. The soil DOM Shannon index, the Pielou

index, and bacterial alpha diversity were significantly positively correlated, indicating that bacterial diversity and soil DOM diversity are interlinked, but not fungal. This finding is supported by Blanchet et al. (2017) who demonstrated that bacterial diversity increased with the addition of DOM from a number of sources [60].

Vegetation restoration played an important role in the chronosequence studied in shaping the soil microbial community, DOM, and soil chemical properties. Soil microbial communities were shaped by changes in soil pH and nutrients driven by vegetation succession. The most likely reasons for the change in DOM composition during vegetation restoration were changing litter composition and microbial utilization preferences. Thieme et al. (2019) attributed the dominance of lignin-like formulae in coniferous forest DOM and lignin- and tannin-like molecules in broadleaved forests to the differing litter composition [36]. A similar conclusion can be drawn from our results. The lignin/CRAM-like structure content in soil DOM at the restored sites was significantly higher than that in the bare land. The lignin/CRAM-like structure content in the broadleaf forest was slightly lower than that in the mixed forest, while the tannin content was significantly higher (Table S2). Lignin/CRAM-like structure molecules are reported to be difficult to decompose due to the barrier formed by these structures around the whole cellulose complex in litter [61]; thus, lignin/CRAM-like structure molecules account for the highest proportion of DOM. Although tannin-like compounds have been reported in high concentrations in the litter and plant litter inputs will have increased over time during vegetation restoration, tannins did not dominate soil DOM, probably because the phenolic content of litter delayed its colonization by decomposers [62]. In addition, tannin has been shown to combine with other substances which increases its persistence [37], and thus it was not easily degraded by microorganisms.

5. Conclusions

The abundance and diversity of soil bacteria increased significantly and gradually stabilized after revegetation, while the diversity of soil fungi increased after revegetation to slightly mature coniferous forests. During vegetation restoration, the diversity and complexity of soil DOM molecules increases, with higher carbon numbers and DBE. The high H/C soil DOM degraded preferentially, while low H/C DOM was recalcitrant during vegetation restoration because organic matter decomposition and utilization preferences of soil microorganisms differ. The soil DOM Shannon index and the Pielou index are significantly and positively correlated with soil bacterial alpha diversity during vegetation restoration. Additionally, the soil microbial community and DOM molecules interact strongly, indicating complex connectivity and strong interactions. As most of the DOM molecules are resistant to change during the restoration chronosequence, vegetation restoration facilitates carbon sequestration in the soil, thereby contributing to climate change mitigation. This study provides further insight into the fate of soil DOM in the revegetation process and its interrelationship with soil microorganisms, and helps to evaluate the functional recovery of degraded ecosystems after revegetation. The non-soluble C in soil also influences the microbial community composition and activity, and thus the interaction of all forms of soil C and microbial interaction needs further study.

Supplementary Materials: The following supporting information can be downloaded at https://www.mdpi.com/article/10.3390/f14020270/s1, Table S1. The stoichiometric ranges used to establish the boundaries of different compound classes; Table S2. Relative abundance (%) of major DOM compound subcategories and classes in soil at different sites after vegetation restoration. Major subcategories are CHO, CHON, and CHOS; major classes are lipids, aliphatic/proteins, lignin/carboxylic rich alicyclic molecules (CRAM)-like structures, carbohydrates, aromatic structures, and tannins; Section S1. Further details of FT-ICR MS methods and data analysis; Section S2. Calculation formulas of DBE, H/C, O/C, m/z, NOSC, the Shannon index, and the Pielou index; Figure S1. Chemical properties of different vegetation type plots during vegetation restoration. Values are means $\pm$ SE (n = 3). Different letters above the bars indicate significant differences ($p < 0.05$) among sites according to the LSD test or Tamhane's T2 test. (a) pH; (b) ammoniacal nitrogen concentration ($NH4^+$); (c)

total nitrogen concentration (TN); (d) total carbon concentration (TC); (e) dissolved organic carbon concentration (DOC); (f) nitrate nitrogen concentration (NO3⁻). Data from Hu et al. (2021); Figure S2. Plots of double bond equivalence (DBE) vs. carbon number of removed, resistant, and produced DOM in soil samples from vegetation restoration sites of different types compared with the control (bare land) site. Points in orange represent DOM molecules that disappeared after vegetation restoration (removed), points in blue represent unchanged DOM molecules (resistant), and points in green represent new molecules that appeared during vegetation restoration (produced); Figure S3. Venn diagrams of soil bacteria (a) and fungi (b) OTUS of different forest types during vegetation restoration. Microbial sequencing data from Hu et al. (2021); Figure S4. Correlation analysis between soil environmental factors and soil bacterial phylum (a), bacterial genus (b), fungal phylum (c), and fungal genus (d). The size of the circle shows the magnitude of the correlation, with orange for a positive correlation and blue for a negative correlation. * represents $p < 0.05$ and ** represents $p < 0.01$. Microbial sequencing data from Hu et al. (2021). References [24,25,63–70] are cited in Supplementary Materials.

References

1. Hu, P.; Raza, S.; Zamanian, K.; Ullah, S.; Kuzyakov, Y.; Virto, I.; Zhou, J. Inorganic carbon losses by soil acidification jeopardize global efforts on carbon sequestration and climate change mitigation. *J. Clean. Prod.* **2021**, *315*, 128036.
2. Deng, L.; Liu, G.B.; Shangguan, Z.P. Land-use conversion and changing soil carbon stocks in China's 'Grain-for-Green'Program: A synthesis. *Glob. Chang. Biol.* **2014**, *20*, 3544–3556. [CrossRef] [PubMed]
3. Liu, H.; Xu, H.; Wu, Y.; Ai, Z.; Zhang, J.; Liu, G.; Xue, S. Effects of natural vegetation restoration on dissolved organic matter (DOM) biodegradability and its temperature sensitivity. *Water Res.* **2021**, *191*, 116792. [CrossRef] [PubMed]
4. Battin, T.J.; Luyssaert, S.; Kaplan, L.A.; Aufdenkampe, A.K.; Richter, A.; Tranvik, L.J. The boundless carbon cycle. *Nat. Geosci.* **2009**, *2*, 598–600. [CrossRef]
5. Roulet, N.; Moore, T.R. Environmental chemistry: Browning the waters. *Nature* **2006**, *444*, 283–284. [CrossRef]
6. Wang, J.J.; Liu, Y.; Bowden, R.D.; Lajtha, K.; Simpson, A.J.; Huang, W.L.; Simpson, M.J. Long-term nitrogen addition alters the composition of soil-derived dissolved organic matter. *ACS Earth Space Chem.* **2019**, *4*, 189–201. [CrossRef]
7. Kalbitz, K.; Kaiser, K. Ecological aspects of dissolved organic matter in soils. *Geoderma* **2003**, *113*, 177–178. [CrossRef]
8. Zhang, K.; Cheng, X.; Shu, X.; Liu, Y.; Zhang, Q. Linking soil bacterial and fungal communities to vegetation succession following agricultural abandonment. *Plant Soil* **2018**, *431*, 19–36. [CrossRef]
9. Lu, J.; Li, S.; Wu, X.; Liang, G.; Gao, C.; Li, J.; Jin, D.; Wang, B.; Zhang, M.; Zheng, F.; et al. The dominant microorganisms vary with aggregates sizes in promoting soil carbon accumulation under straw application. *Arch. Agron. Soil Sci.* **2021**, *69*, 1–17. [CrossRef]
10. Tian, Q.; Taniguchi, T.; Shi, W.Y.; Li, G.; Yamanaka, N.; Du, S. Land-use types and soil chemical properties influence soil microbial communities in the semiarid Loess Plateau region in China. *Sci. Rep.* **2017**, *7*, 45289. [CrossRef]
11. Bourbonniere, R.A.; Creed, I.F. Biodegradability of dissolved organic matter extracted from a chronosequence of forest-floor materials. *J. Plant Nutr. Soil Sci.* **2006**, *169*, 101–107. [CrossRef]
12. Ye, Q.; Wang, Y.H.; Zhang, Z.T.; Huang, W.L.; Li, L.P.; Li, J.; Liu, J.; Zheng, Y.; Mo, J.M.; Zhang, W.; et al. Dissolved organic matter characteristics in soils of tropical legume and non-legume tree plantations. *Soil Biol. Biochem.* **2020**, *148*, 107880. [CrossRef]
13. Guo, X.P.; Chen, H.Y.H.; Meng, M.J.; Biswas, S.R.; Ye, L.X.; Zhang, J.C. Effects of land use change on the composition of soil microbial communities in a managed subtropical forest. *For. Ecol. Manag.* **2016**, *373*, 93–99. [CrossRef]

14. Deng, Q.; Cheng, X.L.; Hui, D.F.; Zhang, Q.; Li, M.; Zhang, Q.F. Soil microbial community and its interaction with soil carbon and nitrogen dynamics following afforestation in central China. *Sci. Total Environ.* **2016**, *541*, 230–237. [CrossRef] [PubMed]
15. Xie, J.; Guo, J.; Yang, Z.; Huang, Z.; Chen, G.; Yang, Y. Rapid accumulation of carbon on severely eroded red soils through afforestation in subtropical China. *For. Ecol. Manag.* **2013**, *300*, 53–59. [CrossRef]
16. Wang, X.; Li, S.; Huang, S.; Cui, Y.; Fu, H.; Li, T.; Zhao, W.; Yang, X. *Pinus massoniana* population dynamics: Driving species diversity during the pioneer stage of ecological restoration. *Glob. Ecol. Conserv.* **2021**, *27*, e01593. [CrossRef]
17. Gao, S.; DeLuca, T.H. Wood biochar impacts soil phosphorus dynamics and microbial communities in organically-managed croplands. *Soil Biol. Biochem.* **2018**, *126*, 144–150. [CrossRef]
18. Jones, D.L.; Willett, V.B. Experimental evaluation of methods to quantify dissolved organic nitrogen (DON) and dissolved organic carbon (DOC) in soil. *Soil Biol. Biochem.* **2006**, *38*, 991–999. [CrossRef]
19. Huang, H.; Jia, Y.; Sun, G.X.; Zhu, Y.G. Arsenic speciation and volatilization from flooded paddy soils amended with different organic matters. *Environ. Sci. Technol.* **2012**, *46*, 2163–2168. [CrossRef]
20. Li, X.M.; Sun, G.X.; Chen, S.; Fang, Z.; Yuan, H.Y.; Shi, Q.; Zhu, Y.G. Molecular chemodiversity of dissolved organic matter in paddy soils. *Environ. Sci. Technol.* **2018**, *52*, 963–971. [CrossRef]
21. Li, X.M.; Chen, Q.; He, C.; Shi, Q.; Chen, S.C.; Reid, B.J.; Zhu, Y.G.; Sun, G.X. Organic carbon amendments affect the chemodiversity of soil dissolved organic matter and its associations with soil microbial communities. *Environ. Sci. Technol.* **2018**, *53*, 50–59. [CrossRef] [PubMed]
22. Shang, H.; Zhu, X.; Shen, M.; Luo, J.; Zhou, S.; Li, L.; Shi, Q.; Zhou, D.; Zhang, S.; Chen, J.; et al. Decarbonylation reaction of saturated and oxidized tar from pyrolysis of low aromaticity biomass boost reduction of hexavalent chromium. *Chem. Eng. J.* **2019**, *360*, 1042–1050. [CrossRef]
23. Chen, Q.L.; An, X.L.; Li, H.; Su, J.Q.; Ma, Y.B.; Zhu, Y.G. Long-term field application of sewage sludge increases the abundance of antibiotic resistance genes in soil. *Environ. Int.* **2016**, *92–93*, 1–10. [CrossRef]
24. Hu, H.Y.; Zhang, Y.L.; Zhu, Z.P.; Huang, C.F.; Wang, S.Z.; Zhou, C.F. Changes in soil enzyme activity and microbial diversity at different vegetation restoration stages in eroded red soil. *Chin. J. Appl. Environ. Biol.* **2021**, *27*, 734–741. (In Chinese) [CrossRef]
25. Smith, C.R.; Sleighter, R.L.; Hatcher, P.G.; Lee, J.W. Molecular characterization of inhibiting biochar water-extractable substances using electrospray ionization Fourier transform ion cyclotron resonance mass spectrometry. *Environ. Sci. Technol.* **2013**, *47*, 13294–13302. [CrossRef] [PubMed]
26. Jiao, S.; Chen, W.; Wang, J.; Du, N.; Li, Q.; Wei, G. Soil microbiomes with distinct assemblies through vertical soil profiles drive the cycling of multiple nutrients in reforested ecosystems. *Microbiome* **2018**, *6*, 146. [CrossRef]
27. Hansell, D.A. Recalcitrant dissolved organic carbon fractions. *Annu. Rev. Mar. Sci.* **2013**, *5*, 421–445. [CrossRef]
28. Vorobev, A.; Sharma, S.; Yu, M.; Lee, J.; Washington, B.J.; Whitman, W.B.; Ballantyne, F.; Medeiros, P.M.; Moran, M.A. Identifying labile DOM components in a coastal ocean through depleted bacterial transcripts and chemical signals. *Environ. Microbiol.* **2018**, *20*, 3012–3030. [CrossRef]
29. Osterholz, H.; Singer, G.; Wemheuer, B.; Daniel, R.; Simon, M.; Niggemann, J.; Dittmar, T. Deciphering associations between dissolved organic molecules and bacterial communities in a pelagic marine system. *ISME J.* **2016**, *10*, 1717–1730. [CrossRef]
30. Riedel, T.; Biester, H.; Dittmar, T. Molecular fractionation of dissolved organic matter with metal salts. *Environ. Sci. Technol.* **2012**, *46*, 4419–4426. [CrossRef]
31. Šantl-Temkiv, T.; Finster, K.; Dittmar, T.; Hansen, B.M.; Thyrhaug, R.; Nielsen, N.W.; Karlson, U.G. Hailstones: A window into the microbial and chemical inventory of a storm cloud. *PLoS ONE* **2013**, *8*, e53550. [CrossRef] [PubMed]
32. Yang, Z.; Wullschleger, S.D.; Liang, L.; Graham, D.E.; Gu, B. Effects of warming on the degradation and production of low molecular-weight labile organic carbon in an Arctic tundra soil. *Soil Biol. Biochem.* **2016**, *95*, 202–211. [CrossRef]
33. Arrieta, J.M.; Mayol, E.; Hansman, R.L.; Herndl, G.J.; Dittmar, T.; Duarte, C.M. Dilution limits dissolved organic carbon utilization in the deep ocean. *Science* **2015**, *348*, 331–333. [CrossRef] [PubMed]
34. Zhang, T.; Zhang, L.; Zhou, Y.; Wei, Q.; Chung, K.H.; Zhao, S.; Xu, C.; Shi, Q. Transformation of nitrogen compounds in deasphalted oil hydrotreating: Characterized by electrospray ionization Fourier transform-ion cyclotron resonance mass spectrometry. *Energy Fuels* **2013**, *27*, 2952–2959. [CrossRef]
35. Dubenok, N.N.; Lebedev, A.V.; Gemonov, A.V. Hydrological Role of Forest Stands in a Small Catchment Basin. *Russ. Agric. Sci.* **2021**, *47*, 323–327. [CrossRef]
36. Thieme, L.; Graeber, D.; Hofmann, D.; Bischoff, S.; Schwarz, M.T.; Steffen, B.; Meyer, U.N.; Kaupenjohann, M.; Wilcke, W.; Michalzik, B.; et al. Dissolved organic matter characteristics of deciduous and coniferous forests with variable management: Different at the source, aligned in the soil. *Biogeosciences* **2019**, *16*, 1411–1432. [CrossRef]
37. Bai, L.L.; Cao, C.C.; Wang, C.H.; Xu, H.C.; Zhang, H.; Slaveykova, V.I.; Jiang, H.L. Toward Quantitative Understanding of the Bioavailability of Dissolved Organic Matter in Freshwater Lake during Cyanobacteria Blooming. *Environ. Sci. Technol.* **2017**, *51*, 6018–6026. [CrossRef]
38. Pharand, B.; Carisse, O.; Benhamou, N. Cytological aspects of compost-mediated induced resistance against Fusarium crown and root rot in tomato. *Phytopathology* **2002**, *92*, 424–438. [CrossRef]
39. Rodríguez, J.; Elissetche, J.P.; Valenzuela, S. Tree endophytes and wood biodegradation. In *Endophytes of Forest Trees*; Springer: Dordrecht, The Netherlands, 2011; pp. 81–93.

40. Osono, T. Role of phyllosphere fungi of forest trees in the development of decomposer fungal communities and decomposition processes of leaf litter. *Can. J. Microbiol.* **2006**, *52*, 701–716. [CrossRef]

41. Schmidt, S.K.; Nemergut, D.R.; Darcy, J.L.; Lynch, R. Do bacterial and fungal communities assemble differently during primary succession? *Mol. Ecol.* **2014**, *23*, 254–258. [CrossRef]

42. Zhang, C.; Liu, G.B.; Xue, S.; Wang, G.L. Soil bacterial community dynamics reflect changes in plant community and soil properties during the secondary succession of abandoned farmland in the Loess Plateau. *Soil Biol. Biochem.* **2016**, *97*, 40–49. [CrossRef]

43. Liu, G.; Chen, L.; Shi, X.; Yuan, L.Y.; Yuan Lock, T.R.; Kallenbach, R.L.; Yuan, Z. Changes in rhizosphere bacterial and fungal community composition with vegetation restoration in planted forests. *Land Degrad. Dev.* **2019**, *30*, 1147–1157. [CrossRef]

44. Li, W.Q.; Huang, Y.X.; Chen, F.S.; Liu, Y.Q.; Lin, X.F.; Zong, Y.Y.; Wu, G.Y.; Yu, Z.R.; Fang, X.M. Mixing with broad-leaved trees shapes the rhizosphere soil fungal communities of coniferous tree species in subtropical forests. *For. Ecol. Manag.* **2021**, *480*, 118664. [CrossRef]

45. Guo, Y.; Hou, L.; Zhang, Z.; Zhang, J.; Cheng, J.; Wei, G.; Lin, Y. Soil microbial diversity during 30 years of grassland restoration on the Loess Plateau, China: Tight linkages with plant diversity. *Land Degrad. Dev.* **2019**, *30*, 1172–1182. [CrossRef]

46. Bautista-Cruz, A.; del Castillo, R.F. Soil changes during secondary succession in a tropical montane cloud forest area. *Soil Sci. Soc. Am. J.* **2005**, *69*, 906–914. [CrossRef]

47. Zhu, C.; Tian, G.L.; Luo, G.W.; Kong, Y.L.; Guo, J.J.; Wang, M.; Guo, S.W.; Ling, N.; Shen, Q.R. N-fertilizer-driven association between the arbuscular mycorrhizal fungal community and diazotrophic community impacts wheat yield. *Agric. Ecosyst. Environ.* **2018**, *254*, 191–201. [CrossRef]

48. Navarrete, A.A.; Venturini, A.M.; Meyer, K.M.; Klein, A.M.; Tiedje, J.M.; Bohannan, B.J.; Nüsslein, K.; Tsai, S.M.; Rodrigues, J.L. Differential response of Acidobacteria subgroups to forest-to-pasture conversion and their biogeographic patterns in the western Brazilian Amazon. *Front. Microbiol.* **2015**, *6*, 1443. [CrossRef]

49. Chen, Z.; Maltz, M.R.; Zhang, Y.; O'Brien, B.J.; Neff, M.; Wang, Y.; Cao, J. Plantations of cinnamomum camphora (Linn) presl with distinct soil bacterial communities mitigate soil acidity within polluted locations in southwest China. *Forests* **2021**, *12*, 657. [CrossRef]

50. Liu, T.; Wu, X.; Li, H.; Ning, C.; Li, Y.; Zhang, X.; He, J.; Filimonenko, E.; Chen, S.; Chen, X.; et al. Soil quality and r–K fungal communities in plantations after conversion from subtropical forest. *Catena* **2022**, *219*, 106584. [CrossRef]

51. Zumsteg, A.; Luster, J.; Göransson, H.; Smittenberg, R.H.; Brunner, I.; Bernasconi, S.M.; Zeyer, J.; Frey, B. Bacterial, archaeal and fungal succession in the forefield of a receding glacier. *Microb. Ecol.* **2012**, *63*, 552–564. [CrossRef]

52. Boye, K.; Noël, V.; Tfaily, M.M.; Bone, S.E.; Williams, K.H.; Bargar, J.R.; Fendorf, S. Thermodynamically controlled preservation of organic carbon in floodplains. *Nat. Geosci.* **2017**, *10*, 415–421. [CrossRef]

53. Follett, C.L.; Repeta, D.J.; Rothman, D.H.; Xu, L.; Santinelli, C. Hidden cycle of dissolved organic carbon in the deep ocean. *Proc. Natl. Acad. Sci. USA* **2014**, *111*, 16706–16711. [CrossRef] [PubMed]

54. Roth, V.-N.; Dittmar, T.; Gaupp, R.; Gleixner, G. The molecular composition of dissolved organic matter in forest soils as a function of pH and temperature. *PLoS ONE* **2015**, *10*, e0119188. [CrossRef] [PubMed]

55. Zhou, C.; Liu, Y.; Liu, C.; Liu, Y.; Malak, M.T. Compositional changes of dissolved organic carbon during its dynamic desorption from hyporheic zone sediments. *Sci. Total Environ.* **2019**, *658*, 16–23. [CrossRef]

56. Zhou, L.; Zhou, Y.Q.; Hu, Y.; Cai, J.; Liu, X.; Bai, C.G.; Tang, X.M.; Zhang, Y.L.; Jang, K.S.; Spencer, R.G.M.; et al. Microbial production and consumption of dissolved organic matter in glacial ecosystems on the Tibetan Plateau. *Water Res.* **2019**, *160*, 18–28. [CrossRef]

57. Bi, B.; Yuan, Y.; Zhang, H.; Wu, Z.; Wang, Y.; Han, F. Rhizosphere soil metabolites mediated microbial community changes of *Pinus sylvestris* var. mongolica across stand ages in the Mu Us Desert. *Appl. Soil Ecol.* **2022**, *169*, 104222. [CrossRef]

58. Zhou, M.; Hu, H.; Wang, J.; Zhu, Z.; Feng, Y. Nitric Acid Rain Increased Bacterial Community Diversity in North Subtropical Forest Soil. *Forests* **2022**, *13*, 1349. [CrossRef]

59. Mao, H.; Wang, K.; Wang, Z.; Peng, J.; Ren, N. Metabolic function, trophic mode, organics degradation ability and influence factor of bacterial and fungal communities in chicken manure composting. *Bioresour. Technol.* **2020**, *302*, 122883. [CrossRef]

60. Blanchet, M.; Pringault, O.; Panagiotopoulos, C.; Lefèvre, D.; Charriere, B.; Ghiglione, J.F.; Fernandez, C.; Aparicio, F.K.; Marassé, C.; Catala, P.; et al. When riverine dissolved organic matter (DOM) meets labile DOM in coastal waters: Changes in bacterial community activity and composition. *Aquat. Sci.* **2017**, *79*, 27–43. [CrossRef]

61. Melillo, J.M.; Aber, J.D.; Linkins, A.E.; Ricca, A.; Fry, B.; Nadelhoffer, K.J. Carbon and nitrogen dynamics along the decay continuum: Plant litter to soil organic matter. *Plant Soil* **1989**, *115*, 189–198. [CrossRef]

62. Yang, Q.; Li, R.; Zhang, W.; Zheng, W.; Wang, Q.; Chen, L.; Guan, X.; Xu, M.; Wang, S. Decomposition of harvest residue needles of different needle ages in a Chinese fir (Cunninghamia lanceolata) plantation. *Plant Soil* **2018**, *423*, 273–284. [CrossRef]

63. Lv, J.; Zhang, S.; Wang, S.; Luo, L.; Cao, D.; Christie, P. Molecular-scale investigation with ESI-FT-ICR-MS on fractionation of dissolved organic matter induced by adsorption on iron oxyhydroxides. *Environ. Sci. Technol.* **2016**, *50*, 2328–2336. [CrossRef] [PubMed]

64. Mesfioui, R.; Love, N.G.; Bronk, D.A.; Mulholland, M.R.; Hatcher, P.G. Reactivity and chemical characterization of effluent organic nitrogen from wastewater treatment plants determined by Fourier transform ion cyclotron resonance mass spectrometry. *Water Res.* **2012**, *46*, 622–634. [CrossRef]

65. Xu, C.; Chen, H.; Sugiyama, Y.; Zhang, S.; Li, H.P.; Ho, Y.F.; Chuang, C.Y.; Schwehr, K.A.; Kaplan, D.I.; Yeager, C.; et al. Novel molecular-level evidence of iodine binding to natural organic matter from Fourier transform ion cyclotron resonance mass spectrometry. *Sci. Total Environ.* **2013**, *449*, 244–252. [CrossRef] [PubMed]
66. Bhatia, M.P.; Das, S.B.; Longnecker, K.; Charette, M.A.; Kujawinski, E.B. Molecular characterization of dissolved organic matter associated with the Greenland ice sheet. *Geochim. Cosmochim. Acta* **2010**, *74*, 3768–3784. [CrossRef]
67. Chen, H.; Stubbins, A.; Perdue, E.M.; Green, N.W.; Helms, J.R.; Mopper, K.; Hatcher, P.G. Ultrahigh resolution mass spectrometric differentiation of dissolved organic matter isolated by coupled reverse osmosis-electrodialysis from various major oceanic water masses. *Mar. Chem.* **2014**, *164*, 48–59. [CrossRef]
68. Ohno, T.; He, Z.; Sleighter, R.L.; Honeycutt, C.W.; Hatcher, P.G. Ultrahigh resolution mass spectrometry and indicator species analysis to identify marker components of soil-and plant biomass-derived organic matter fractions. *Environ. Sci. Technol.* **2010**, *44*, 8594–8600. [CrossRef] [PubMed]
69. LaRowe, D.E.; Van Cappellen, P. Degradation of natural organic matter: A thermodynamic analysis. *Geochim. Cosmochim. Acta* **2010**, *75*, 2030–2042. [CrossRef]
70. Noriega-Ortega, B.E.; Wienhausen, G.; Mentges, A.; Dittmar, T.; Simon, M.; Niggemann, J. Does the chemodiversity of bacterial exometabolomes sustain the chemodiversity of marine dissolved organic matter? *Front. Microbiol.* **2019**, *10*, 215. [CrossRef] [PubMed]